Strong modification of thin film properties due to screening across the interface

S. G. Altendorf,[1] A. Reisner,[1] B. Tam,[1,2] F. Meneghin,[1,3] S. Wirth,[1] and L. H. Tjeng[1]
[1]*Max Planck Institute for Chemical Physics of Solids, Nöthnitzer Strasse 40, 01187 Dresden, Germany*
[2]*University of British Columbia, Vancouver, British Columbia, Canada V6T 1Z4*
[3]*Politecnico di Milano, Piazza Leonardo da Vinci, 32, 20133 Milano, Italy*

(Received 14 December 2017; published 17 April 2018)

We report on our investigation of the influence of screening across the interface on the properties of semiconducting thin films. Using EuO as a well-defined model material, layers of various thickness deposited on yttria-stabilized zirconia (100) substrates were covered half with Mg metal and half with the wide-band-gap insulator MgO. We observed that the Curie temperature for the thinnest films is significantly higher for the part which is interfaced with the metal compared to the part which is interfaced with the insulator. We infer that the proximity of a polarizable medium reduces the energies of virtual charge excitations and thus increases the effective exchange interactions, a strong effect that can be utilized systematically for the design of thin film and multilayer systems.

DOI: 10.1103/PhysRevB.97.165422

I. INTRODUCTION

When interfacing two materials, new physical properties can emerge at the interface which can be very different from the properties of each of the connected materials. A famous example is the interface of $LaAlO_3$ and $SrTiO_3$, which was observed to be metallic although the two materials separately are insulators [1,2]. The behavior at interfaces can be significantly modified through the effects of local symmetry breaking, charge transfer, electrostatic coupling, strain, and frustration [3–8]. This wide range of parameters offers a tremendous opportunity for fundamental as well as applied sciences.

In view of the vast amount of research activities on thin films and interfaces, it is surprising that the influence of screening effects near the interface has received little attention so far. Using the insightful image-charge-screening model, Duffy and Stoneham [9] were able to argue that the energies for virtual charge excitations in a material can be strongly reduced in proximity of a highly polarizable medium. Indeed, spectroscopically it was shown that the band gap in semiconductors or insulators, as well as the on-site Coulomb repulsion (Hubbard U) and the charge-transfer energies in transition metal oxides, are significantly reduced when placed close to a metal [10–13]. This may explain, for example, why few monolayers of NiO order antiferromagnetically on a metallic substrate but not on a wide-gap insulating substrate [14].

The presence of screening across the interface is a very pressing topic, especially in view of the recent activities in constructing interfaces between topological insulators on one side and superconducting or ferromagnetic adlayers on the other side [15–17]. The band gap of the topological insulator is then expected to be influenced by the near presence of the metallic adlayer. In case a semiconducting ferromagnet is being applied as an adlayer, then one may also expect reversely that its magnetic properties should be affected by the typically high polarizability of the topological insulator material.

In this work, we focus on the question of how a change in the dielectric constant of an adjacent medium influences the magnetic properties of a semiconducting material. We select europium monoxide (EuO), one of the rare ferromagnetic semiconductors [18], as the material of choice. EuO is an extensively studied material because of its unprecedented properties, which include huge magneto-optical effects [19,20], a metal insulator transition in the Eu-rich compound that can exceed 13 orders of magnitude [21], and a nearly 100% spin-polarized conduction band at low temperature [22–24]. Although having a relatively low bulk Curie temperature of 69 K, it is an ideal model system for our study because of its large magnetic moment of $7\mu_B$ per Eu ion and its well-established and well-controlled thin film preparation route [25,26].

We investigate the effect of screening by interfacing EuO layers of various thickness with metallic Mg and the wide-band-gap insulating MgO, i.e., we are contrasting the influence of an adjacent medium with an infinitely large dielectric constant with one having a dielectric constant of about 3 only. The EuO films were grown on insulating yttria-stabilized cubic zirconia (YSZ) (100) substrates and then half their surface was covered with Mg metal and the other half with MgO. In this way, one can ensure that the EuO for both interfaces is grown under the same conditions, i.e., the two parts of the sample have the same EuO composition and thickness. Moreover, an additional influence of different substrate strain on the Curie temperature is avoided. With EuO being a high-moment ferromagnet, the magnetic properties of the films can be straightforwardly measured using a standard superconducting quantum interference device (SQUID).

II. EXPERIMENT

The EuO thin films as well as the Mg and MgO layers were prepared by molecular beam epitaxy under ultra-high-vacuum conditions with base pressures in the low 10^{-10} mbar range. EuO films of thicknesses between ∼1–10 nm were grown

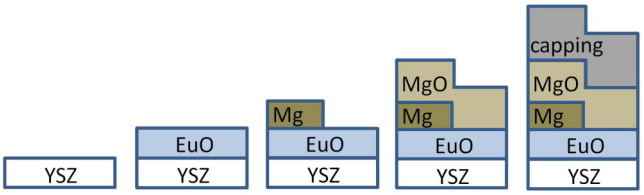

FIG. 1. Schematic sketch of the thin film stack (not to scale).

using the well-established Eu-distillation method, described in more detail in Refs. [25] and [26]. High-purity Eu metal was evaporated from an effusion cell at rates of about 7–8 Å/min ($T_{\mathrm{Eu}} \approx 560^{\circ}$ C) in a molecular oxygen atmosphere of 2.5–3.5 $\times$ 10^{-8} mbar. The substrate temperature was set to 400° C–420° C during growth to reevaporate/distill the excess Eu. As substrates, single-crystalline, epi-polished YSZ substrates with (100) surface were used, which were annealed for at least 2 h at 600° C in an oxygen atmosphere of 5 $\times$ 10^{-7} mbar prior to deposition. The small lattice mismatch of only 0.4% allows for an epitaxial EuO growth.

After the EuO deposition, half of the film surface was covered with a shadow mask and about 20-nm Mg metal was deposited onto the uncovered half of the EuO at rates of 4–6 Å/min ($T_{\mathrm{Mg}} \approx 260^{\circ}$ C–300° C). The substrate was kept at room temperature to prevent chemical reactions with the EuO. In the next step, the mask was removed to deposit an about 20-nm-thick MgO layer onto the whole structure. The MgO deposition was started by first opening the Mg shutter and then, after 40 s, opening the oxygen leak valve to 8–10 $\times$ 10^{-8} mbar to prevent an overoxidation of the EuO layer. After the *in situ* characterization of the structural and chemical properties, the films were covered with a capping layer of about 100 Å thickness to protect the air-sensitive EuO during *ex situ* measurements. Aluminum, chromium, or gold was used as a capping layer. We did not observe any significant difference in the magnetization measurements for the various capping materials. A sketch of the architecture of the thin film stack is shown in Fig. 1.

The crystalline growth of the EuO films was verified during deposition by reflection high-energy electron diffraction (RHEED) using a STAIB Instruments EK-35-R system. Afterwards, all samples were analyzed *in situ* by photoelectron spectroscopy using a Scienta R3000 electron energy analyzer at 1486.6 eV photon energy (monochromatized Al $K\alpha$ light) in normal emission geometry at room temperature with an overall energy resolution set to about 0.4 eV. The magnetic properties were studied *ex situ* by SQUID measurements using a Quantum Design MPMS-XL5 magnetometer. *Ex situ* x-ray reflectivity (XRR) measurements were carried out in a high-resolution Philips X'Pert MRD diffractometer using monochromatic Cu $K\alpha 1$ radiation to verify the thickness of the layers.

III. GROWTH

In Fig. 2 exemplary images of the RHEED measurements on an annealed YSZ (100) substrate [Fig. 2(a)] and the deposited layers are shown. The sharp diffraction streaks in Fig. 2(b) reveal that the EuO films grow epitaxially on the YSZ (100)

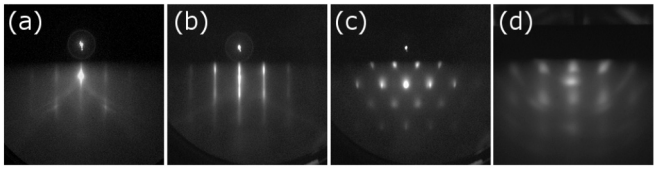

FIG. 2. RHEED images of (a) annealed YSZ (001) substrate, (b) EuO on YSZ (001), (c) EuO on YSZ (001) covered with a thin layer of Mg metal, and (d) EuO on YSZ (001) covered with a thin layer of MgO. The electron energy was set to 15 keV with the beam incident along the [100] direction.

substrates. As can bee seen in Figs. 2(c) and 2(d), the Mg metal and MgO layers grow in an island (spotty pattern) or partly polycrystalline (blurry diffraction pattern with rings) fashion on the EuO films due to lattice mismatch and low substrate temperature ($T_{\mathrm{sub}} \approx 20^{\circ}$ C–40° C) during deposition. The distance of the RHEED streaks of the MgO layer indicates that the MgO is fully relaxed with a lattice constant of about the bulk value $a_{\mathrm{MgO}} = 4.21$ Å. No influence of strain on the EuO films is expected for both adlayers. For the EuO deposition, RHEED intensity oscillations were observed (not shown here), which are a signature of a smooth layer-by-layer growth (see Ref. [26]) and allow for an estimation of the EuO thickness. The Mg, MgO, and capping layer thicknesses are deduced from the flux rates as measured using a quartz crystal microbalance. Additionally, x-ray reflectivity measurements were performed for the calibration of the thickness, which confirms the results determined by RHEED oscillations and microbalance.

IV. PHOTOEMISSION

Since EuO could be oxygen deficient or further oxidized to form Eu^{3+} compounds, it is very important to prove that the quality of the EuO layer is not influenced by the deposition of Mg metal and MgO. Therefore, we performed photoelectron spectroscopy measurements at various Mg and MgO adlayer thicknesses and we present the results in Figs. 3 and 4.

Figure 3(a) shows the valence-band spectrum of the pristine EuO film with the typical sharp $Eu^{2+}4f$ states at about 2 eV binding energy, the O $2p$ feature at 5 eV, and the Eu $5p$ peak at 18 eV. When depositing thin layers of Mg metal onto this film, the shape and the position of these EuO structures do not change, verifying that the EuO remains intact upon metal deposition. For larger Mg thicknesses, an additional peak at 13 eV binding energy becomes apparent. This peak can be assigned to an 11-eV plasmon peak from the $Eu^{2+}4f$ at 2 eV binding energy due to the presence of the Mg adlayer, as we can show using core-level spectroscopy. Figure 3(b) displays the Eu $4d$ level together with the Mg $2s$ and $2p$. We can observe that the Mg $2s$ and $2p$ of the Mg-covered EuO films have multiple satellite structures at 11 eV energy intervals, identical to those of a Mg metal film. This establishes that the 11-eV satellite structures are plasmon peaks and therefore also that the Mg adlayer is truly metallic. We can observe, furthermore, that the Eu $4d$ levels of the pristine EuO film and the Mg-covered EuO film are identical, confirming again that the EuO film is not altered upon Mg coverage.

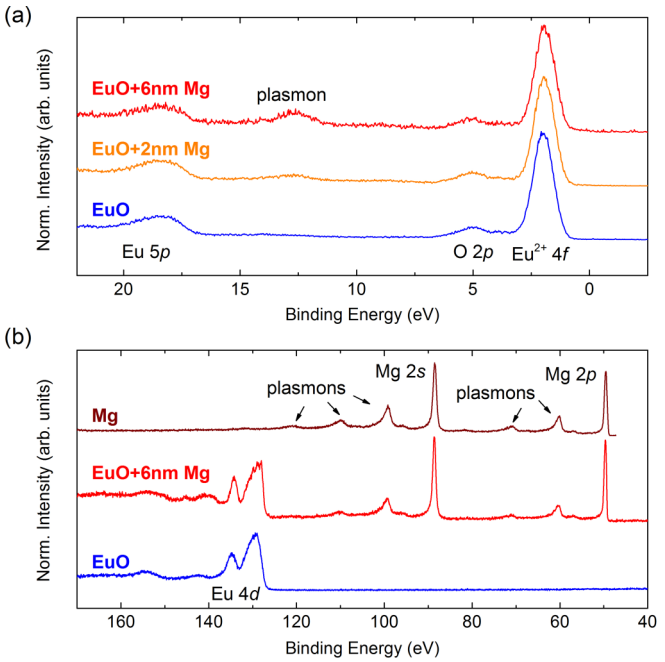

FIG. 3. XPS valence-band and core-level spectra of EuO covered with thin layers of Mg metal. Spectra of EuO and Mg metal are shown for comparison: (a) valence band and (b) Eu $4d$ – Mg $2s + 2p$ core levels.

Now we focus on the deposition of MgO on EuO. The results are presented in Fig. 4. The spectra in Fig. 4(a) show the evolution of the valence band when MgO is deposited onto the EuO film. Also for the MgO overlayer, the Eu $4f$ peak does not reveal any changes. This verifies that the deposition of the

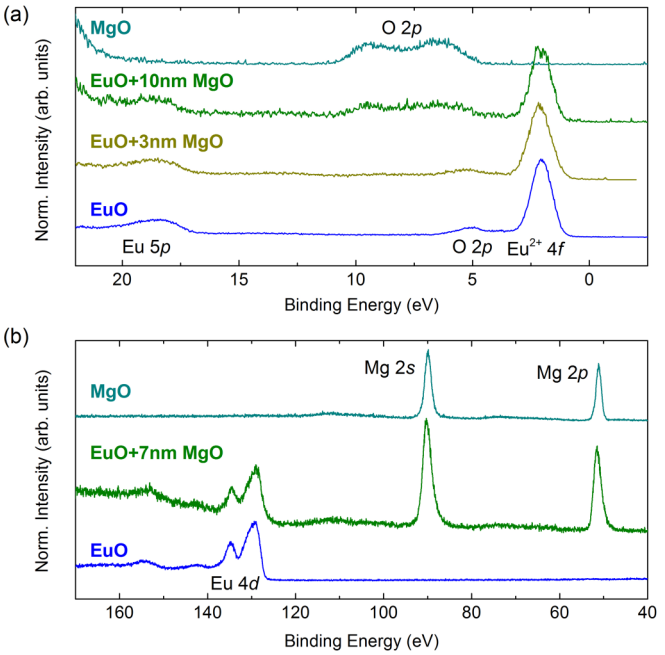

FIG. 4. XPS valence-band and core-level spectra of EuO covered with thin layers of MgO. Spectra of EuO and MgO are shown for comparison: (a) valence band and (b) Eu $4d$ – Mg $2s + 2p$ core levels.

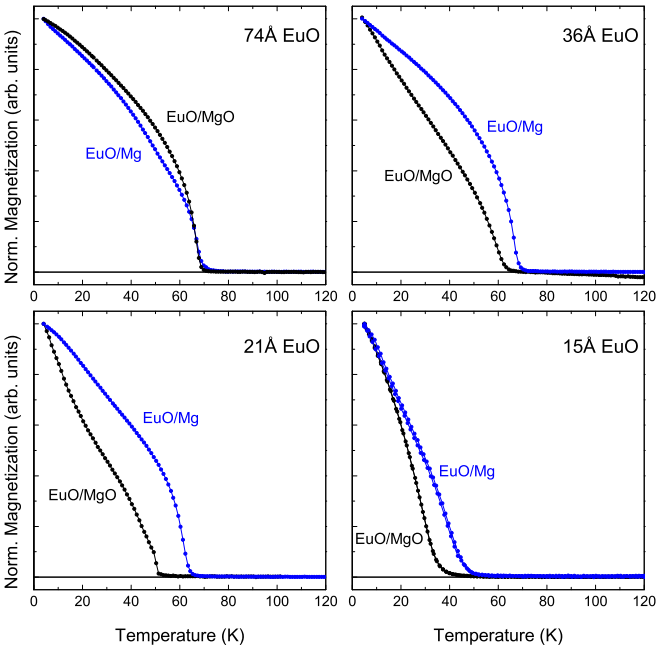

FIG. 5. Temperature-dependent magnetization curves of EuO interfaced with Mg metal (blue) and MgO (black) for EuO thicknesses of 74, 36, 21, and 15 Å. The applied magnetic field was set to 50 G.

oxide layer does not cause a degradation of the EuO layer. For larger thicknesses, the O $2p$ band of the MgO becomes visible at 5–10 eV binding energy. The valence-band spectrum as well as the Mg $2s$ and $2p$ core-level spectra in Fig. 4(b) do not show any satellite features, i.e., no excitations that can be identified as plasmons. This establishes the absence of any metallic Mg and verifies that all the deposited Mg is being completely oxidized to form the wide-band-gap insulating MgO.

V. MAGNETIC PROPERTIES

Having shown that the growth procedures yield well-defined EuO-Mg/MgO layer structures, we now study their magnetic properties. For the SQUID measurements, the samples were cut using a sapphire blade to separate them into parts with EuO/Mg and EuO/MgO interfaces. Figure 5 shows some exemplary temperature-dependent magnetization curves. For a film with 74 Å thickness, the Curie temperature is measured to be 69 K for EuO interfaced with both Mg and MgO. This agrees with the T_C of bulk EuO. For an EuO film of 36 Å thickness, T_C is still 69 K for the Mg-covered side. However, for the MgO-covered side, the transition temperature is lowered to 63 K. For the even smaller thicknesses of 21 and 15 Å, T_C is decreased also for the Mg-interfaced EuO but remains significantly higher than the respective part covered by MgO.

The influence of finite-size effects on the properties of EuO films has been shown previously, such as thickness-dependent changes in the transport properties [27] or in the size of the energy gap [28]. In particular, the decrease of the magnetic ordering temperature for ultrathin EuO layers was predicted by theoretical calculations [29–32] and has been also investigated in several experimental studies [27,33–35]. Our data show an additional important aspect: the lowering of the Curie

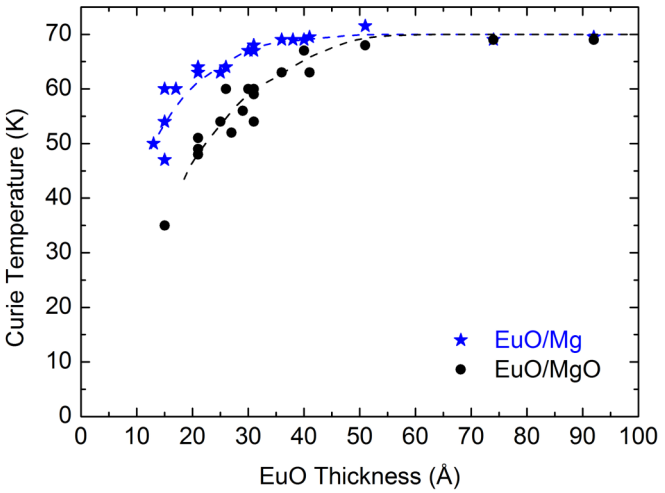

FIG. 6. Curie temperatures for EuO interfaced with Mg metal (blue) and MgO (black) for various EuO thicknesses. The dashed lines serve as a guide to the eye.

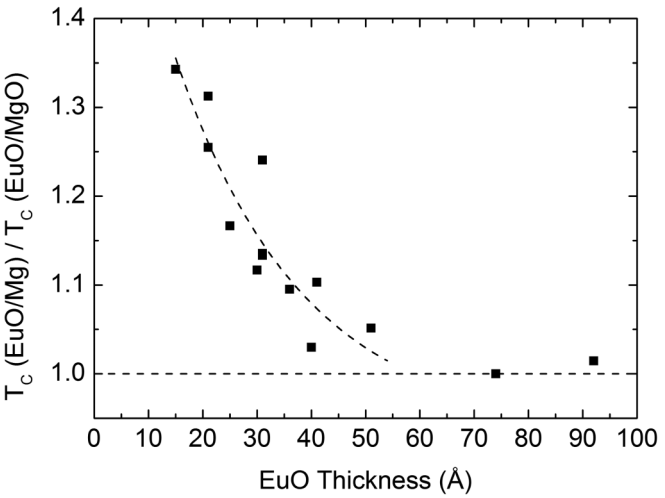

FIG. 7. Ratios of the Curie temperatures for EuO interfaced with Mg metal and MgO for various EuO thicknesses. The respective data were measured on pairs of sample pieces of the same EuO thin film. The dashed line serves as a guide to the eye.

temperature for a given ultrathin EuO film not only depends on its layer thickness but is also strongly influenced by the material in proximity. One can clearly see that T_C is significantly higher for the sample pieces with the EuO/Mg metal interface compared to the pieces with the EuO/MgO interface.

In Fig. 6, the Curie temperatures of all investigated EuO thin films of various thicknesses covered with Mg metal and MgO are summarized. The data show that a lowering of the magnetic ordering temperature in thin EuO films sets in for a thickness of around 50 Å for EuO films interfaced with MgO but only for smaller thicknesses below about 35 Å when interfaced with Mg metal. The observed scattering of the results is possibly caused by degradation effects at the edges of the EuO layer during the *ex situ* SQUID measurements and uncertainties in the determination of the EuO thickness. On average, however, the data points show a clear trend. In the ultra-thin-film limit, the magnetic ordering temperature of EuO is higher when interfaced with Mg metal compared to insulating MgO. The significance of the effect of the metallic adlayer becomes even more evident if one considers the ratios of the Curie temperatures of the EuO interfaced with Mg and MgO, respectively, as shown in Fig. 7. For the about 20-Å-thick EuO films, the ratio is about 1.3, and the trend is that this ratio increases further and more rapidly for smaller thicknesses.

VI. DISCUSSION

The results fit nicely with the ideas put forward by Duffy and Stoneham [9]. Films, equally thin but interfaced by different materials, can have indeed quite different properties. In terms of the image-charge-screening model, Mg metal provides a much better screening than the wide-gap insulator MgO. Since screening is also strongly distance dependent, it would be interesting to quantify how the band gap of EuO actually develops as a function of the distance to the interface. Theoretical calculations are therefore highly desired. Standard band structure calculations, however, will not be adequate, since screening energies are quadratic with charge and therefore cannot be captured in terms of one-electron potentials. Instead one has to resort to computationally more demanding approaches such as the GW [36,37] to describe the charge excitation energies properly. In any case, one can infer that any form of reduction of the band gap leads to a lowering of (virtual) charge excitation energies, which can generally induce an increase of the exchange interaction strength ($J_{ex} \propto t^2/U$, $J_{\text{superex}} \propto [-2t^4/\Delta^2][(1/\Delta) + (1/U)]$, in which U is the on-site Coulomb interaction as defined in the Hubbard model, Δ the charge-transfer energy, and t the transfer integral) and thus also enhance the magnetic ordering temperatures of magnetic semiconductors or insulators [10–13]. We would like to note that since the coherence length of the magnetization is much larger than the thickness of the ultrathin films, thermodynamically the whole thin film layer is expected to have only one common Curie temperature [31,32,38].

Ruderman-Kittel-Kasuya-Yosida (RKKY) interactions can be ruled out to dominate the properties of the insulating EuO layers. They are present only directly at the Mg interface where the localized Eu 4f states and the metallic conduction electrons overlap. Our study, however, shows that the Curie temperatures are enhanced even in 30–40-Å-thick EuO films. Screening effects, having a $1/r$ spacial dependence, influence a larger volume of the EuO layer.

VII. CONCLUSIONS

To summarize, by comparing ultrathin EuO films interfaced with Mg metal and insulating MgO, we have shown that the ferromagnetic ordering temperature is significantly higher for the EuO/metal interface at a given EuO thickness. The finite-size effects are considerably compensated in the proximity of the highly polarizable metal. Our results indicate that the screening by a metallic adlayer can indeed significantly change the properties of a semiconducting thin film material and point out the importance of considering the dielectric properties of each layer when designing a nanoscale heterostructure device.

ACKNOWLEDGMENTS

We gratefully acknowledge P. Thalmeier for fruitful discussions. We thank T. Mende and C. Becker for their skillful technical assistance during the experiments. This work was partially supported by the Deutsche Forschungsgemeinschaft (DFG) through Schwerpunktprogramm (SPP) 1666.

[1] A. Ohtomo and H. Y. Hwang, Nature (London) **427**, 423 (2004).
[2] J. Mannhart, D. H. A. Blank, H. Y. Hwang, A. J. Millis, and J.-M. Triscone, MRS Bull. **33**, 1027 (2008).
[3] D. G. Schlom, L.-Q. Chen, X. Pan, A. Schmehl, and M. A. Zurbuchen, J. Am. Ceram. Soc. **91**, 2429 (2008).
[4] P. Zubko, S. Gariglio, M. Gabay, P. Ghosez, and J.-M. Triscone, Annu. Rev. Condens. Matter Phys. **2**, 141 (2011).
[5] J. Chakhalian, A. J. Millis, and J. Rondinelli, Nat. Mater. **11**, 92 (2012).
[6] K. R. Poeppelmeier and J. M. Rondinelli, Nat. Chem. **8**, 292 (2016).
[7] M. O'Sullivan, J. Hadermann, M. S. Dyer, S. Turner, J. Alaria, T. D. Manning, A. M. Abakumov, J. B. Claridge, and M. J. Rosseinsky, Nat. Chem. **8**, 347 (2016).
[8] F. Hellman, A. Hoffmann, Y. Tserkovnyak, G. S. D. Beach, E. E. Fullerton, C. Leighton, A. H. MacDonald, D. C. Ralph, D. A. Arena, H. A. Dürr *et al.*, Rev. Mod. Phys. **89**, 025006 (2017).
[9] D. M. Duffy and A. M. Stoneham, J. Phys. C: Solid State Phys. **16**, 4087 (1983).
[10] R. Hesper, L. H. Tjeng, and G. A. Sawatzky, Europhys. Lett. **40**, 177 (1997).
[11] S. Altieri, L. H. Tjeng, F. C. Voogt, T. Hibma, and G. A. Sawatzky, Phys. Rev. B **59**, R2517 (1999).
[12] S. Altieri, L. H. Tjeng, and G. A. Sawatzky, Thin Solid Films **400**, 9 (2001).
[13] S. Altieri, L. H. Tjeng, F. C. Voogt, T. Hibma, O. Rogojanu, and G. A. Sawatzky, Phys. Rev. B **66**, 155432 (2002).
[14] S. Altieri, M. Finazzi, H. H. Hsieh, M. W. Haverkort, H.-J. Lin, C. T. Chen, S. Frabboni, G. C. Gazzadi, A. Rota, S. Valeri, and L. H. Tjeng, Phys. Rev. B **79**, 174431 (2009).
[15] P. Zareapour, A. Hayat, S. Y. F. Zhao, M. Kreshchuk, A. Jain, D. C. Kwok, N. Lee, S.-W. Cheong, Z. Xu, A. Yang, G. D. Gu, S. Jia, R. J. Cava, and K. S. Burch, Nat. Commun. **3**, 1056 (2012).
[16] E. Wang, H. Ding, A. V. Fedorov, W. Yao, Z. Li, Y.-F. Lv, K. Zhao, L.-G. Zhang, Z. Xu, J. Schneeloch, R. Zhong, S.-H. Ji, L. Wang, K. He, X. Ma, G. Gu, H. Yao, Q.-K. Xue, X. Chen, and S. Zhou, Nat. Phys. **9**, 621 (2013).
[17] F. Katmis, V. Lauter, F. S. Nogueira, B. A. Assaf, M. E. Jamer, P. Wei, B. Satpati, J. W. Freeland, I. Eremin, D. Heiman, P. Jarillo-Herrero, and J. S. Moodera, Nature (London) **533**, 513 (2016).
[18] B. T. Matthias, R. M. Bozorth, and J. H. Van Vleck, Phys. Rev. Lett. **7**, 160 (1961).
[19] H.-Y. Wang, J. Schoenes, and E. Kaldis, Helv. Phys. Acta **59**, 102 (1986).
[20] K. Y. Ahn and M. W. Shafer, J. Appl. Phys. **41**, 1260 (1970).
[21] J. B. Torrance, M. W. Shafer, and T. R. McGuire, Phys. Rev. Lett. **29**, 1168 (1972).
[22] P. G. Steeneken, L. H. Tjeng, I. Elfimov, G. A. Sawatzky, G. Ghiringhelli, N. B. Brookes, and D.-J. Huang, Phys. Rev. Lett. **88**, 047201 (2002).
[23] A. Schmehl, V. Vaithyanathan, A. Herrnberger, S. Thiel, C. Richter, M. Liberati, T. Heeg, M. Röckerath, L. F. Kourkoutis, S. Mühlbauer, P. Böni, D. A. Muller, Y. Barash, J. Schubert, Y. Idzerda, J. Mannhart, and D. G. Schlom, Nat. Mater. **6**, 882 (2007).
[24] R. P. Panguluri, T. S. Santos, E. Negusse, J. Dvorak, Y. Idzerda, J. S. Moodera, and B. Nadgorny, Phys. Rev. B **78**, 125307 (2008).
[25] P. G. Steeneken, Ph.D. thesis, Rijksuniversiteit Groningen, 2002.
[26] R. Sutarto, S. G. Altendorf, B. Coloru, M. Moretti Sala, T. Haupricht, C. F. Chang, Z. Hu, C. Schüßler-Langeheine, N. Hollmann, H. Kierspel, H. H. Hsieh, H.-J. Lin, C. T. Chen, and L. H. Tjeng, Phys. Rev. B **79**, 205318 (2009).
[27] M. Müller, G.-X. Miao, and J. S. Moodera, J. Appl. Phys. **105**, 07C917 (2009).
[28] G. M. Prinz, T. Gerber, A. Lorke, and M. Müller, Appl. Phys. Lett. **109**, 202401 (2016).
[29] R. Schiller and W. Nolting, Solid State Commun. **110**, 121 (1999).
[30] R. Schiller and W. Nolting, Phys. Rev. Lett. **86**, 3847 (2001).
[31] W. Nolting and C. Santos, Phys. Status Solidi B **236**, 272 (2003).
[32] R. Rausch and W. Nolting, J. Phys.: Condens. Matter **21**, 376002 (2009).
[33] T. S. Santos, J. S. Moodera, K. V. Raman, E. Negusse, J. Holroyd, J. Dvorak, M. Liberati, Y. U. Idzerda, and E. Arenholz, Phys. Rev. Lett. **101**, 147201 (2008).
[34] M. Barbagallo, T. Stollenwerk, J. Kroha, N.-J. Steinke, N. D. M. Hine, J. F. K. Cooper, C. H. W. Barnes, A. Ionescu, P. M. D. S. Monteiro, J.-Y. Kim, K. R. A. Ziebeck, C. J. Kinane, R. M. Dalgliesh, T. R. Charlton, and S. Langridge, Phys. Rev. B **84**, 075219 (2011).
[35] A. Melville, T. Mairoser, A. Schmehl, T. Birol, T. Heeg, B. Holländer, J. Schubert, C. J. Fennie, and D. G. Schlom, Appl. Phys. Lett. **102**, 062404 (2013).
[36] J. B. Neaton, M. S. Hybertsen, and S. G. Louie, Phys. Rev. Lett. **97**, 216405 (2006).
[37] J. D. Sau, J. B. Neaton, H. J. Choi, S. G. Louie, and M. L. Cohen, Phys. Rev. Lett. **101**, 026804 (2008).
[38] T. Takeda and H. Fukuyama, J. Phys. Soc. Jpn. **40**, 925 (1976).